Title
ELECTROCHEMISTRY OF IODIDE IN PROPYLENE CARBONATE. II. THEORETICAL MODEL

Author
Hanson, K.J.

Publication Date
1986-10-01

LBL-22009
Preprint

Lawrence Berkeley Laboratory
UNIVERSITY OF CALIFORNIA

Materials & Molecular Research Division

Submitted to Journal of the
Electrochemical Society

ELECTROCHEMISTRY OF IODIDE IN PROPYLENE CARBONATE. II. THEORETICAL MODEL

K.J. Hanson, M.J. Matlosz,
J. Newman, and C.W. Tobias

October 1986

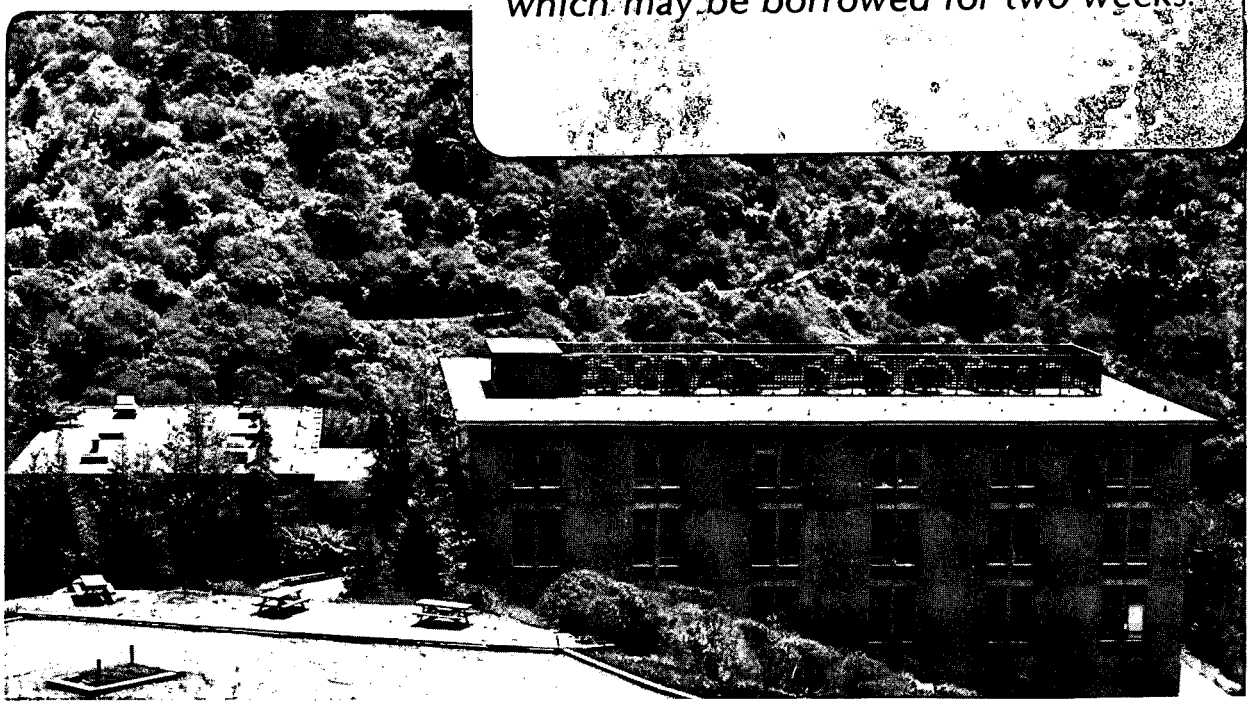

Prepared for the U.S. Department of Energy under Contract DE-AC03-76SF00098

DISCLAIMER

ELECTROCHEMISTRY OF IODIDE IN PROPYLENE CARBONATE
II. THEORETICAL MODEL

K.J. Hanson*, Michael J. Matlosz**, John Newman and Charles W. Tobias

Materials and Molecular Research Division
Lawrence Berkeley Laboratory
and Department of Chemical Engineering
University of California
Berkeley, CA 94720

ABSTRACT

An algorithm based on Duhamel's superposition integral is used to simulate cyclic voltammograms for iodide electrochemistry on platinum in propylene carbonate. The electrochemistry is represented by the reaction sequence

$$3I^- \rightarrow I_3^- + 2e^- \qquad \text{I}$$

$$2I_3^- \rightarrow 3I_2 + 2e^- \qquad \text{II}$$

where reaction I is rate-limited (Butler-Volmer kinetics) and reaction II is reversible (Nernst equilibrium behavior). Since the nonunity stoichiometries and Butler-Volmer kinetics in the reaction sequence prohibit the use of analytical solution techniques, the superposition-integral algorithm is used as a fast and accurate method for the numerical simulation. The simulated voltammograms for the iodide system agree very well with experimental observations and support the proposed reaction sequence.

---

*Present address: AT&T Bell Laboratories, Murray Hill, NJ 07974

**Present address: Swiss Federal Inst. of Technology, Lausanne, Switzerland

Key words: cyclic voltammetry, simultaneous reactions

1. Introduction

The electrochemical oxidation of iodide in propylene carbonate (PC) is an example of a reaction sequence that is difficult to interpret using classic models of cyclic voltammetry. Although a rich literature is available concerning the theory of cyclic voltammetry for cases of 1:1 reaction stoichiometry, and for reversible electrode reactions, or for Tafel kinetics,[1] the complexity of the iodide system does not permit a straightforward application of these existing analytic solutions. For the interpretation of the iodide system, numerical solutions of the model equations for multiple-reaction systems with nonunity stoichiometries and interdependent reaction rates are required. For this purpose, an algorithm based on the superposition principle (Duhamel's integral) was developed to simulate the voltammogram of the iodide system in PC.

The model is based upon pure diffusion of three species, I^-, I_2, I_3^-, in the electrolytic solution and generalized Butler-Volmer kinetics for rate-limited electrochemical reactions. The solution of these equations for a triangular-wave applied potential gives a simulated voltammetric response for a given solution concentration, sweep rate, and potential scan.

The fact that both electrochemical reactions have a non-unity stoichiometry was a strong incentive to approach the problem numerically. Although Shuman[2][3] has treated the cases of 1:2 and 1:3 reactions, his results are limited to reversible kinetics and single, not sequential, reactions. Since the governing equations for this problem are linear, the surface concentrations of each reactant can be determined using a simple algorithm to evaluate

Duhamel's superposition integral. This technique has recently been applied to other electrochemical problems[4][5] and in certain applications can significantly improve the speed and accuracy of the calculation compared to finite-difference methods.

2. Problem Specification

The reaction mechanism of iodide electrochemistry in PC was derived from cyclic voltammetry experiments of dilute iodide in supported PC solutions using a platinum working electrode and a thallium/thallium iodide reference electrode. These experiments are described in detail in Part I of this series.[6]

Two reactions occur in the anodic sweep,

$$3\,I^- \rightarrow I_3^- + 2\,e^- \qquad \text{(I)}$$

$$2\,I_3^- \rightarrow 3\,I_2 + 2\,e^-. \qquad \text{(II)}$$

At low potential, triiodide is formed according to reaction I. At a more positive potential, the triiodide is oxidized further to iodine by reaction II. Both reactions are chemically "reversible," in the sense that two peaks are observed in both the forward and reverse scans. Reaction II, however, obeys equilibrium (Nernst) behavior at scan rates below 500 mV/s, since the shape and position of the anodic and cathodic peaks are independent of sweep rate in this range. Reaction I is kinetically limited, since the shape and position of the current peaks depend strongly on the sweep rate.

The starting point for a mathematical description of the voltammetric response of this system is Fick's second law, which describes the mass transfer of each species i in the electrolyte under pure diffusion control:

$$\frac{\partial c_i}{\partial t} = D_i \frac{\partial^2 c_i}{\partial x^2}. \qquad (1)$$

In this case three species are considered, I^-, I_2, and I_3^-. The flux of each species to the electrode surface is proportional to the derivative of the concentration at the surface and is equal to the

rate of reaction of that species. Three coupled equations describe the surface concentrations of the three reactants. First, by the restriction that there be no accumulation of any iodide species at the electrode surface (such as by adsorption), a balance on iodine atoms at the electrode surface yields the following flux relation:

$$D_{I^-} \frac{\partial c_{I^-}}{\partial x} + 2 D_{I_2} \frac{\partial c_{I_2}}{\partial x} + 3 D_{I_3^-} \frac{\partial c_{I_3^-}}{\partial x} = 0. \tag{2}$$

Second, the partial current density for reaction I, i_I , is related to the surface concentration of I^- and I_3^-, and to the applied cell potential, by the Butler-Volmer equation,

$$i_I = i_{o,ref} \left[\left(\frac{c_{I^-}}{c_{ref}} \right)^3 \exp\left[\frac{(1-\beta) n_I F \eta_I}{RT} \right] - \left(\frac{c_{I_3^-}}{c_{ref}} \right) \exp\left[\frac{-\beta n_I F \eta_I}{RT} \right] \right]. \tag{3}$$

Since the iodide ion participates only in reaction I, the flux of iodide at the electrode surface is determined directly from this partial current and stoichiometry:

$$D_{I^-} \frac{\partial c_{I^-}}{\partial x} = \frac{3}{n_I F} i_I \, . \tag{4}$$

The total overpotential, η_I, is defined as the difference between the electrode potential and the potential of a reference electrode of the same kind. For this system, η_I is given by

$$\eta_I = V - \Phi_{ref} - \Delta\Phi_{ohm} - U_{I,ref} , \tag{5}$$

where $\Delta\Phi_{ohm}$ represents the ohmic drop and the term $U_{I,ref}$ corrects the reference electrode potential of thallium amalgam/thallium iodide to the potential of the iodide/triiodide reaction at concentration c_{ref} for both reactants. The reference concentration c_{ref} was chosen to be the concentration of iodide in the bulk of the solution. In most cases, the total cell current was very small, and the ohmic term was insignificant.

For reaction I, the exchange current density, $i_{o,ref}$, is based on the reference concentration, c_{ref}, for both I^- and I_3^-, and $U_{I,ref}$ is related to the standard cell potential U_I^o (with respect to TlI/Tl(Hg); saturated thallium amalgam[7]) according to the Nernst equation,

$$U_{I,ref} = U_I^o + \frac{RT}{n_I F}\left[\ln\frac{c_{I_3^-,ref}}{\rho_o} - 3\ln\frac{c_{I^-,ref}}{\rho_o}\right] \tag{6}$$

or

$$U_{I,ref} = U_I^o - \frac{2RT}{n_I R}\ln\left[\frac{c_{ref}}{\rho_o}\right]$$

where ρ_o is the density of the pure solvent (PC) in units of kg/cm^3.

Third, because reaction II exhibits nearly reversible behavior, the potential $(V - \Phi_{ref})$ is related directly to the surface concentrations of iodine and triiodide by the Nernst equation for reaction II:

$$(V - \Phi_{ref}) - \Delta\Phi_{ohm} = U_{II}^o + \frac{RT}{n_{II}F}\ln\frac{c_{I_2}^{\ 3}}{\rho_o c_{I_3^-}^{\ 2}}, \tag{7}$$

where c_{I_2} and $c_{I_3^-}$ are surface concentrations of iodine and triiodide, respectively. In principle, a Butler-Volmer expression could be used to describe this reaction in place of the Nernst expression. In that case, an arbitrarily high exchange-current density chosen for reaction II would simulate the reversible behavior of equation (7).

In triangular-wave voltammetry, the applied potential, $V - \Phi_{ref}$, is swept linearly at a rate of b volts per second. For an anodic sweep starting at an initial potential, $(V - \Phi_{ref})_{min}$,

$$V - \Phi_{ref} = (V - \Phi_{ref})_{min} + bt_a. \tag{8}$$

For a cathodic sweep, starting at $(V - \Phi)_{max}$,

$$V - \Phi_{ref} = (V - \Phi_{ref})_{max} - bt_c. \tag{9}$$

where t_a and t_c are times into an anodic or cathodic sweep, respectively.

The problem specification is completed by setting the initial ($t = 0$) concentration of I^- equal to its bulk value c_{ref} everywhere in solution. The initial concentrations of I_2 and I_3^- can be determined from equilibrium (Nernst) equations for reactions I and II and the initial potential.

3. Application of Duhamel's Superposition Integral

Since the Fick's law expression for the mass-transfer of each species is linear (equation 1), the flux to the electrode surface resulting from any arbitrary (including nonlinear) surface boundary conditions can be obtained by superposing the flux contributions resulting from a succession of simple step changes in concentration at the surface. An illustration of the principle is shown in Figure 1. The concentration gradient rises initially at the beginning of each step in concentration, but the effect of a particular step at future time is damped as the response decays. In the limit of an infinite number of small step changes in surface concentration, the flux resulting from the combination of all these changes is represented by Duhamel's integral,[8]

$$\frac{\partial c_i}{\partial x}(0,t) = \int_0^t \left[\frac{\partial c_i}{\partial t}(0,\tau) \frac{\partial \theta_i}{\partial x}(0,t-\tau) \right] d\tau, \tag{10}$$

where θ_i is the dimensionless concentration resulting from a unit step change in surface concentration. Thus, the surface flux as a function of time is calculated from the integral of the response of the surface flux to a unit step change in surface concentration, multiplied by the time variation of the surface concentration. The advantage of this approach is that flux profiles from complicated, nonlinear surface conditions can be determined by a simple integral equation involving the concentration field arising from a step change, a problem for which an analytic solution is generally available.

In our case, the response to a unit step change in concentration for a semi-infinite stagnant medium is

$$\theta_i = 1 - \frac{2}{\sqrt{\pi}} \int_0^{\xi} \exp(-\xi^2) d\xi, \tag{11}$$

where

$$\xi = \frac{x}{\sqrt{4 D_i t}}. \tag{12}$$

Thus,

$$\frac{\partial \theta_i}{\partial x}(0, t - \tau) = \frac{-1}{\sqrt{\pi D_i (t - \tau)}}. \tag{13}$$

4. Solution Technique

The application of this integral for linear problems and its approximation by a finite sum have been addressed by Wagner[9] and by Acrivos and Chambré[10] and is reviewed by Matlosz.[11] The procedure for using the superposition integral to calculate the surface concentrations and surface fluxes is not direct, since a set of coupled nonlinear functions must be satisfied. At a given step, the values of both the surface concentrations and surface fluxes of all species are unknown and must be determined.

To solve this set of coupled equations, a multi-dimensional Newton-Raphson procedure is used. The nonlinear equations are linearized in a Taylor series expansion about a set of trial values for the surface concentrations. The derivatives needed for the expansion are obtained from the equations by numerical differentiation. New values of the concentrations are obtained from the linearized equations by matrix inversion, and the resulting concentrations are used as new trial values. This procedure is repeated until the resulting concentrations no longer differ from the trial values. Once the surface concentrations and surface fluxes are known, the total current density to the electrode is determined at each potential to simulate the voltammogram.

5. Concentration Profiles

Although the full spatial variation of concentration of each species as a function of time is not required to simulate the voltammogram, the change in the concentration profiles through the course of a single sweep gives a physical picture of the process. The concentration variation of each species in the electrolyte as a function of time can be calculated from Duhamel's integral using the calculated surface concentrations. Figure 2, for example, shows the concentration profiles of I^- for a single reaction, $3I^- \rightarrow I_3^- + 2e^-$, at various times during the first sweep of a voltammetry experiment at 100 mV/s. The initial concentration of iodide is uniform

throughout the solution (curve 1). As the reaction proceeds, the concentration of I^- drops at the electrode surface (curve 2), the boundary layer moves out into solution, and the surface concentration approaches zero (curve 3). When the direction of the potential scan is reversed, the production of iodide at the surface gives a profile having a minimum with a steep gradient at the surface (curve 4). Provided the cathodic switching potential is sufficiently negative and no other reactions occur, the position of the concentration minimum moves away from the surface as the experiment proceeds, and the concentration of iodide at the surface reaches its starting value (curve 5). If the potential is again reversed (as in cyclic voltammetry), the concentration profile of iodide would become "S-shaped."

The presence of these complicated concentration profiles in stagnant solutions during a voltammetry experiment demonstrates how the shape of the voltammogram depends upon each of the experimental parameters, including the sweep rate and the reversal potentials. For example, a faster sweep rate would result in steeper concentration gradients at the surface (and thus higher currents), and the depletion region near the electrode would be relatively narrow.

6. Comparison of Model Voltammograms to Experiment

The parameters used in the simulation are listed in Table 1. Of this set, only the values for $i_{o,ref}$ and β were adjusted. The diffusion coefficient of iodide in PC was measured by potential step experiments, as shown in Part I of this series. In the absence of other measured values, the diffusion coefficients of all other iodine species were assumed to be equal. The values for U^o given by L'Her et al.[12] have been adjusted to give the correct peak separation between reactions I and II. By assuming that the value for iodide oxidation (I) is correct, values of 865 mV and 1265 mV (vs. TlI/Tl(Hg)) for U_I^o and U_{II}^o, respectively were obtained. Independent measurements of the exchange current density ($i_{o,ref}$) and the symmetry coefficient (β) of reaction I in PC were not available. These parameters, therefore, were adjusted. Since reaction II exhibits essentially reversible behavior, the Nernst equation for that reaction is used rather than a Butler-Volmer expression, and no additional parameters are introduced.

A comparison of a calculated voltammogram to experiment, based on the parameters listed in Table 1, is shown in Figure 3. The most serious error appears near the end of the anodic sweep, a discrepancy which is probably due to unsubtracted background currents from the supporting-electrolyte solution.

The sensitivity of the model to $i_{o,ref}$ and β is shown in Figures 4 and 5. When the exchange-current density for reaction I is very large (reversible kinetics), the anodic and cathodic peak separation is 52 mV (the reversible limiting value for a 1:3 reaction stoichiometry[2]), and the widths of the cathodic and anodic peaks are identical. As the exchange-current density decreases, the anodic peak moves in the positive (anodic) direction, whereas the reverse peak becomes broadened and shifted in the negative direction. The relationship between the accuracy of the value of U_f° and the choice of the value for $i_{o,ref}$ is apparent here; a decrease in the value of the exchange-current density decreases the peak separation between reactions I and II. Thus poor correspondence between the observed and simulated peak separation could result from an inaccurate value of either U_f° or $i_{o,ref}$. Figure 5 shows the same simulation for various values of β. A symmetry coefficient of 0.5 yields narrow, closely spaced anodic and cathodic peaks. As the value of β is reduced, a larger fraction of the applied potential promotes the anodic reaction, and the cathodic peak is shifted and broadened accordingly.

7. Simulated Sweep-Rate Behavior

Figures 6 and 7 show the model simulation of the experiments given in Figures 4 and 5 in Part I. The $\Delta\Phi_{ohm}$ term included in the model was used to account for the higher ohmic drop associated with experiments done in the larger cell. The simulation does not track the experimental curves exactly, because the experiment was done in a cell having a different geometry from the cell used to obtain data for fitting the model parameters. Nevertheless, the model fairly closely describes the shape of the voltammograms, including the cathodic shift of peak I′.

An interesting bump or slight peak appears on the simulation shown in Figure 6 at 0.8 V in the cathodic sweep (negative current, lower curve) in advance of the main triiodide reduction wave (peak I′). This "bump" is not a numerical artifact, and it cannot indicate any chemistry more complicated or different from that assumed in the first place.

The current at any given time is the sum of all the partial currents. There is an anodic component of the current from the reaction $3I^- \rightarrow I_3^- + 2e^-$ making a positive contribution from about 1.2 to 1.0 V. The curve goes close to zero around $E = 1$ V, because there is a balance between the anodic contribution from that reaction and a cathodic contribution from the reaction of I_2 back to I_3^-. When the potential reaches $\sim$ 0.9 V, the anodic current shuts off, and the current drops to a more negative value (due to iodine reduction) and shows the plateau or "additional peak." When the potential reaches $\sim$ 0.7 V, the cathodic current from triiodide reduction begins, giving the corresponding reduction wave at $\sim$ 0.5 V. It is delayed, compared to the cessation of anodic current from that reaction, because the kinetics of Reaction I′ are inhibited. Thus the combination of the mass-transfer of two reactions with the slow kinetic step for the first reaction produces the apparent bump. If this appeared on an experimental cyclic voltammogram, it might be misjudged as an impurity or perhaps as an "intermediate."

8. Discussion

The parameters given in Table 1 are not necessarily a unique set. The fit shown here was made by considering the precision with which each of the parameters is known. Small changes in a single parameter, such as the diffusion coefficient, alter the entire voltammogram. To obtain a quantitative understanding of the sensitivity of the simulation to all of these parameters, a multi-variable regression analysis would have to be conducted. Because the model includes several simplifying assumptions (migration and convection effects are neglected, for example), such an extension of the analysis is probably not warranted.

9. Conclusions

A numerical model describing the behavior of an iodide solution in propylene carbonate during cyclic voltammetry experiments is presented. The simulation describes the sequential reaction of iodide to triiodide, followed by oxidation of the triiodide; both electrochemical reactions have a nonunity stoichiometry. Duhamel's superposition integral is used to calculate surface concentrations of the electrochemical species. A comparison of simulated voltammograms to experiment supports the proposed reaction mechanism.

Acknowledgement

This work was supported by the Assisstant Secretary of Conservation and Renewable Energy, Office of Energy Systems Research, Energy Storage Division of the U.S. Department of Energy under contract DE-AC03-76SF00098.

Table 1. Values of Parameters for Model Calculations

$D_{I^-} = 2.0 \times 10^{-6}$ cm^2/s	$T = 298.15$ °K
$D_{I_2} = 2.0 \times 10^{-6}$ cm^2/s	$\rho_o = 1.20 \times 10^{-3}$ kg/cm^3
$D_{I_3^-} = 2.0 \times 10^{-6}$ cm^2/s	$\kappa = 0.2$ mho/cm
	$A = 0.0571$ cm^2
$c_{I^-}{}^o = 2.5 \times 10^{-6}$ mol/cm^3	$(V - \Phi_{ref})_{\min} = 0.4$V
$c_{I_2}{}^o = 8.8 \times 10^{-23}$ mol/cm^3	$(V - \Phi_{ref})_{\max} = 1.8$V
$c_{I_3^-}{}^o = 1.1 \times 10^{-17}$ mol/cm^3	$b = 0.1$ V/s
$n_I = 2$	$n_{II} = 2$
$U_I^o = 0.600$V	$U_{II^o} = 1.265$V
$\beta = 0.2$	
$i_{o,ref} = 6.5 \times 10^{-5}$ A/cm^2	
$c_{I^-,ref} = 2.5 \times 10^{-6}$ mol/cm^3	
$c_{I_3^-,ref} = 2.5 \times 10^{-6}$ mol/cm^3	
$U_{I,ref} = 0.754$V	

All potentials are vs. TlI/saturated Tl(Hg).

List of Symbols

A	Surface area of electrode, cm^2
b	Sweep rate, V/s
c_i	Concentration of species i, mol/cm^3
$c_{i,ref}$	Reference concentration of species i, mol/cm^3
c_i^o	Bulk (or initial) concentration of species i, mol/cm^3
D_i	Diffusion coefficient of species i, cm^2/s
F	Faraday constant, 96487 C/equiv.
$i_{o,ref}$	Exchange-current density of reaction I at reference concentration, A/cm^2
i_I	Partial current of reaction I, A/cm^2
n_I	Charge number of reaction I
n_{II}	Charge number of reaction II
R	Universal gas constant, 8.314 J/mol-K
t	Time, s
t_a	Time into anodic sweep, s
t_c	Time into cathodic sweep, s
T	Temperature, K

U_I^o, U_{II}^o Standard electrode potential of reaction I or II, (all concentrations 1 molal) with respect to TlI/Tl(Hg), V

$U_{I,ref}$ Equilibrium electrode potential of reaction I, (at reference concentration c_{ref}) with respect to TlI/Tl(Hg), V

$V - \Phi_{ref}$ Electrode potential relative to a TlI/Tl(Hg) electrode in the electrolyte solution, V

$(V - \Phi_{ref})_{min}$ Potential at start of anodic sweep, V

$(V - \Phi_{ref})_{max}$ Potential at start of cathodic sweep, V

x Distance from the electrode surface, cm

β Symmetry coefficient for reaction I

$\Delta\Phi_{ohm}$ Ohmic potential in the electrolyte solution, V

η_I Overpotential term in the kinetic expression for reaction I, V

θ_I Concentration response to a unit change in surface concentration, (dimensionless)

K Electrolyte conductivity, mho/cm

ξ Dimensionless distance, $\frac{x}{\sqrt{4D_i t}}$

ρ_o Solvent density, kg/cm^3

τ Variable of integration in Duhamel's integral, s

FIGURE CAPTIONS

Figure 1. Illustration of the principle of superposition.

Figure 2. Concentration profiles of iodide during the first voltammetric sweep. Only the reaction $3I^- \rightarrow I_3^- + 2e^-$ is considered. The initial concentration (curve 1) is uniform. Concentration profiles are shown before (curves 2 and 3) and after (curves 4 and 5) the anodic switching potential $b = 0.1$V/s.

Figure 3. Comparison of model voltammograms to experiment. Parameter values and operating conditions are shown in Table 1.

Figure 4. Sensitivity of simulation to the value of $i_{o,ref}$. β is constant at 0.2 for each curve. Values of other parameters are included in Table 1.

Figure 5. Sensitivity of simulation to the value of β. The exchange current is constant for each curve.

Figure 6. Simulation of iodide voltammetry in PC as a function of the sweep rate. Other model parameters are included in Table 1.

Figure 7. Simulation of iodide voltammetry in PC as a function of the sweep rate. Other model parameters are included in Table 1.

REFERENCES

1. (A) A. J. Bard and L. R. Faulkner, *Electrochemical Methods*, J. Whiley & Sons, Inc., New York (1980). (B) R. S. Nicholson and I. Shain, *Analytical Chemistry, 36*, 706-723 (1964). (C) Z. Galus, *Fundamentals of Electrochemical Analysis*, John Wiley & Sons, Inc, London (1976).

2. M. S. Shuman, *Anal. Chem., 41*, 1, 142 (1969).

3. M. S. Shuman, *Anal. Chem., 42*, 4, 521 (1970).

4. P. C. Andricacos and P. N. Ross, *J. Electrochemical Society, 130*, 1340 (1983).

5. M. Verbrugge and C. W.Tobias, *J. Electrochem. Soc., 132*, 6, 1298 (1985).

6. K. J. Hanson and C. W. Tobias, *J. Electrochem. Soc.* XX, XX (1986).

7. F. G. Baucke and C. W. Tobias, *J. Electrochem. Soc. 116*, 1 (1969).

8. F. B. Hildebrand, *Advanced Calculus for Applications*, pp. 463-467, Prentice Hall, Englewood Cliffs, N.J. (1976).

9. C. Wagner, *J. Mathematical Physics, 32*, 289 (1954).

10. A. Acrivos and P.L.Chambré, *Ind. and Eng. Chem. Fund., 49*, 1025 (1957).

11. M. J. Matlosz, *Experimental Methods and Software Tools For the Analysis of Electrochemical Systems*, Thesis, Dept. of Chem. Eng., Univ. of California, Berkeley, CA. (1985).

12. M. L'Her, D. Morin-Bozec, and J. Courtot-Coupez, *Electroanal. Chem. and Interfacial Electrochem., 61*, 99 (1975).

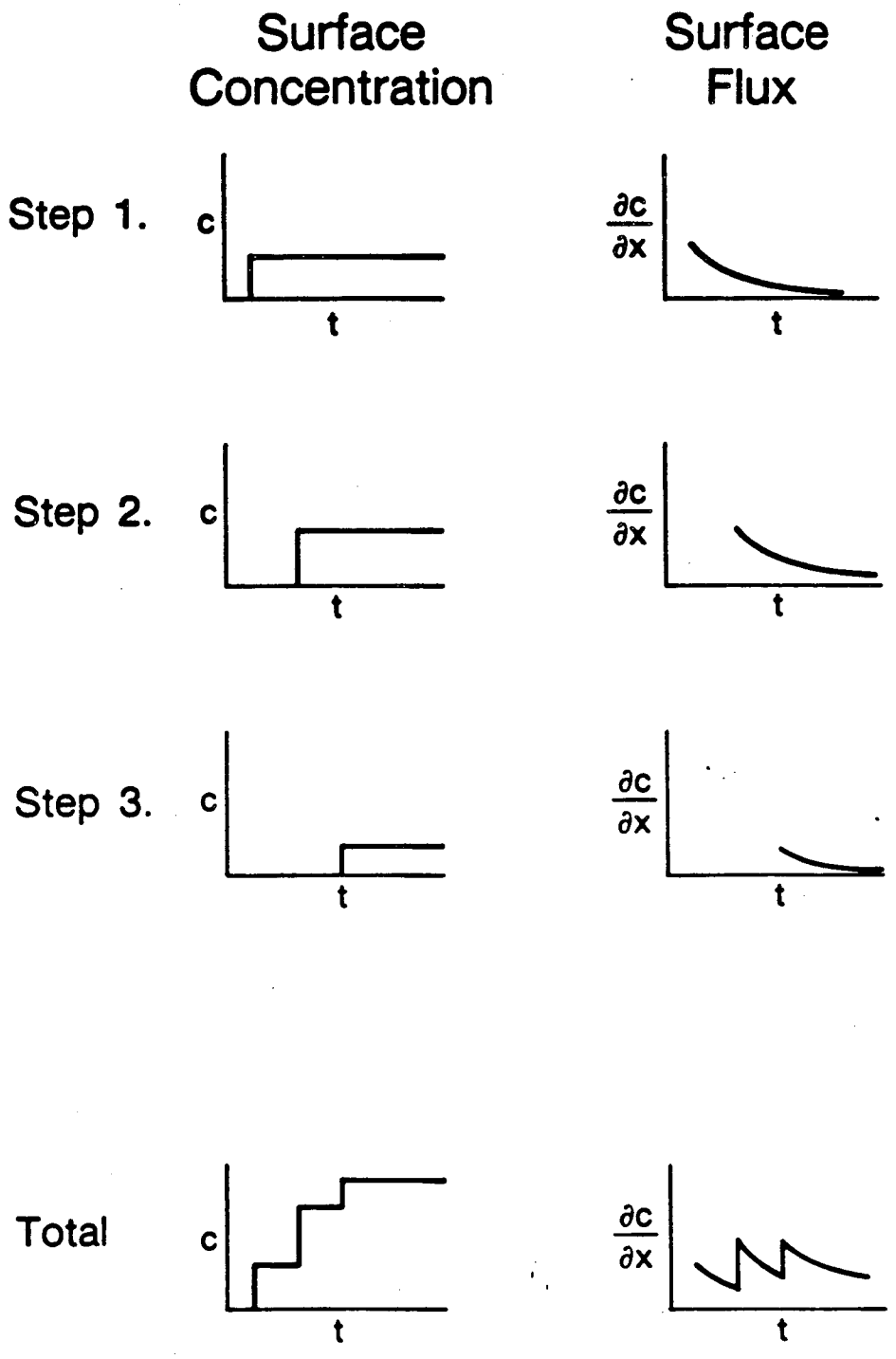
Surface Concentration
Surface Flux
Step 1.
Step 2.
Step 3.
Total
c
t
∂c/∂x
t
XBL 852 8196

FIGURE 1

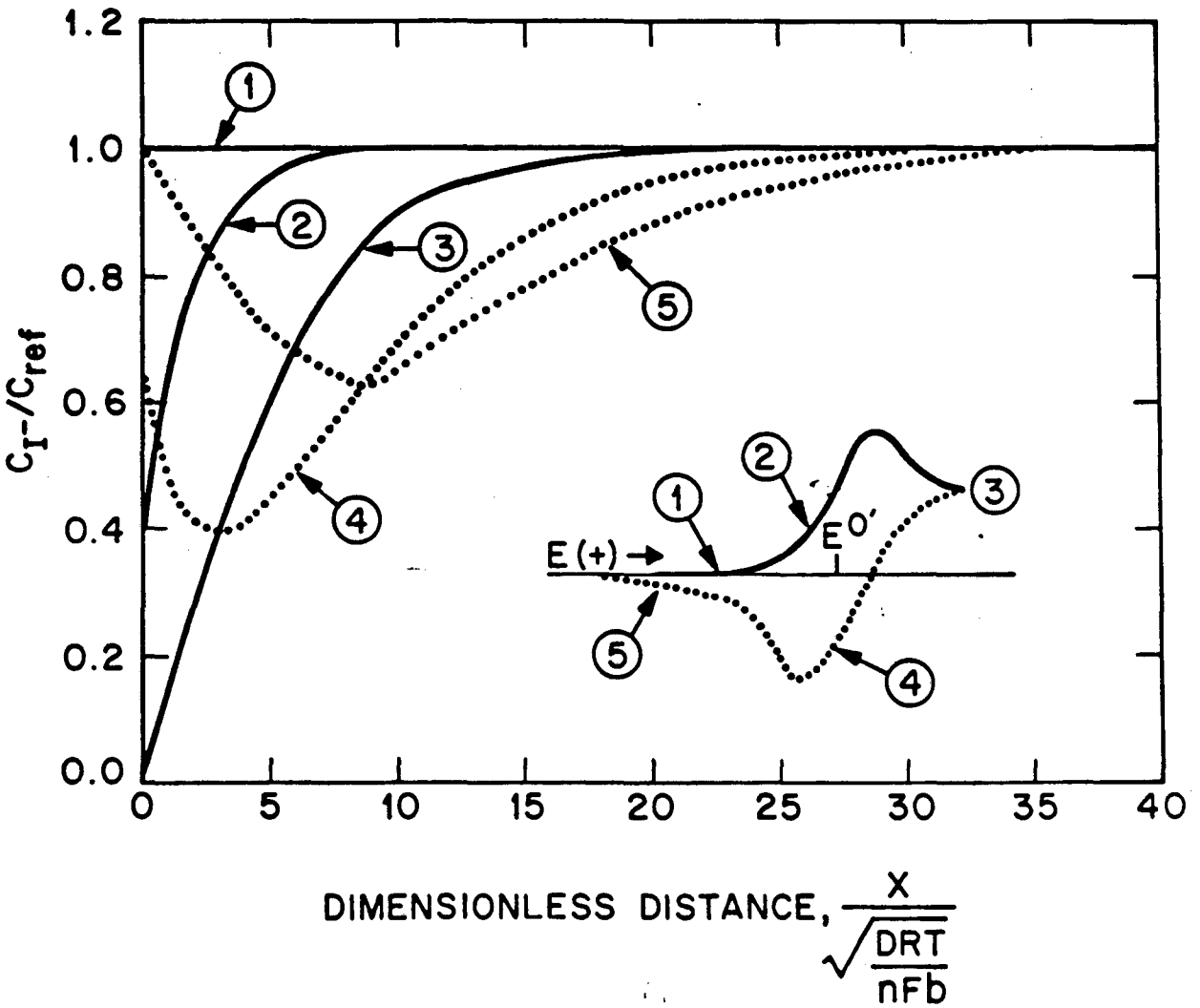
1.2
1.0
0.8
0.6
0.4
0.2
0.0
C_{I^-}/C_{ref}
0
5
10
15
20
25
30
35
40
DIMENSIONLESS DISTANCE, $\frac{X}{\sqrt{\frac{DRT}{nFb}}}$
1
2
3
4
5
E(+)
$E^{0'}$

FIGURE 2

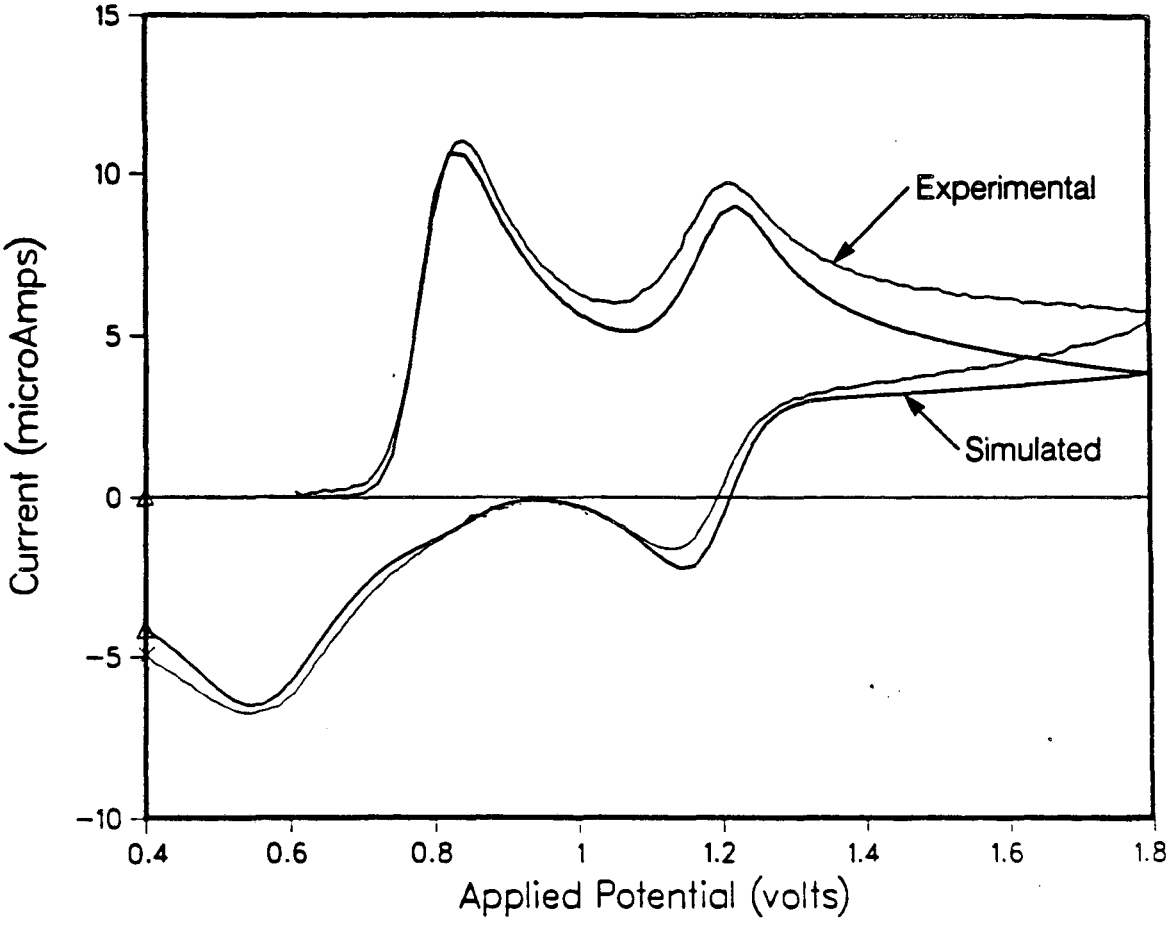
15
10
5
0
−5
−10
0.4
0.6
0.8
1
1.2
1.4
1.6
1.8
Current (microAmps)
Applied Potential (volts)
Experimental
Simulated
XBL 847-7739

FIGURE 3

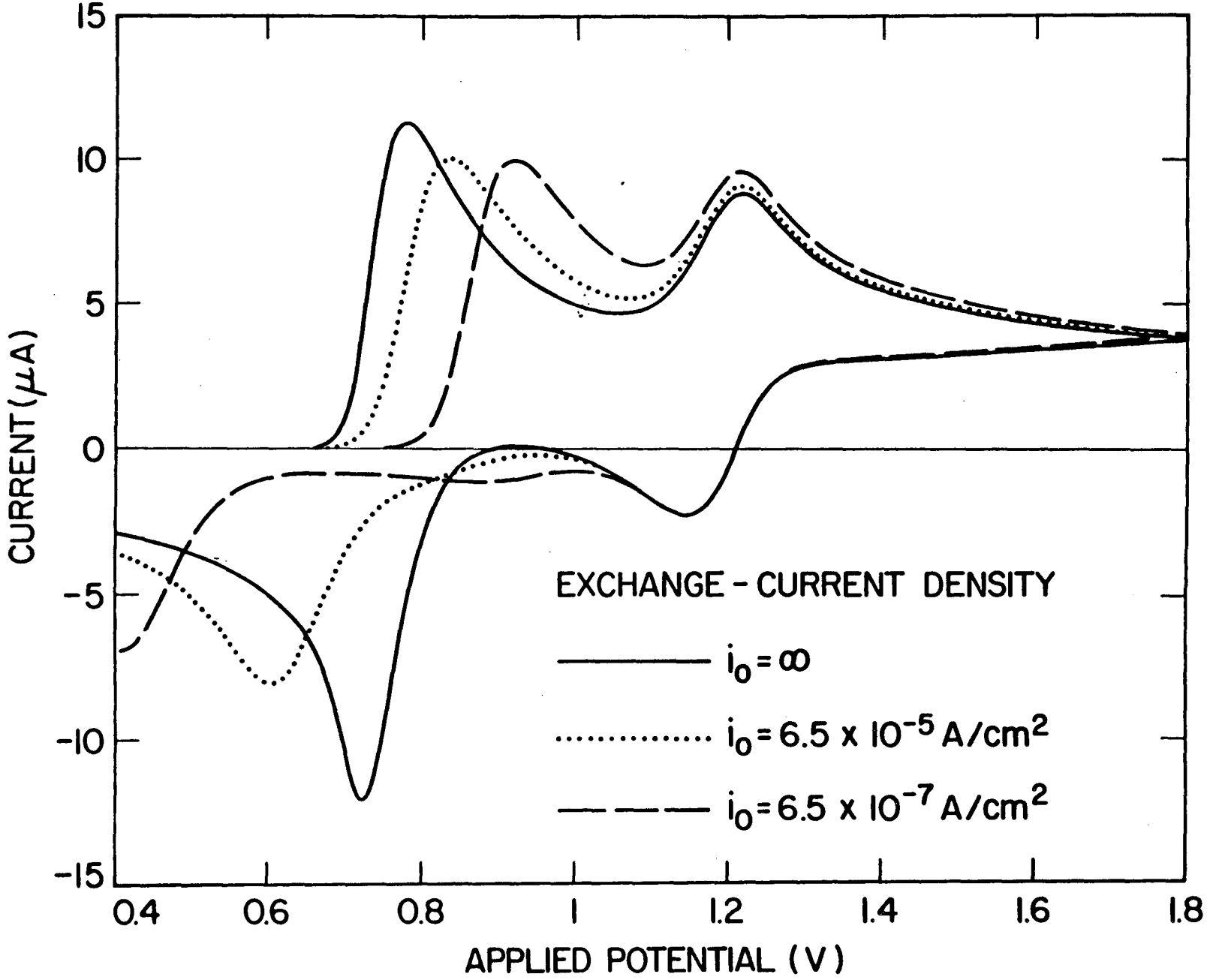
15
10
5
0
-5
-10
-15
CURRENT (μA)
0.4
0.6
0.8
1
1.2
1.4
1.6
1.8
APPLIED POTENTIAL (V)
EXCHANGE - CURRENT DENSITY
$i_0 = \infty$
$i_0 = 6.5 \times 10^{-5}$ A/cm^2
$i_0 = 6.5 \times 10^{-7}$ A/cm^2

FIGURE 4

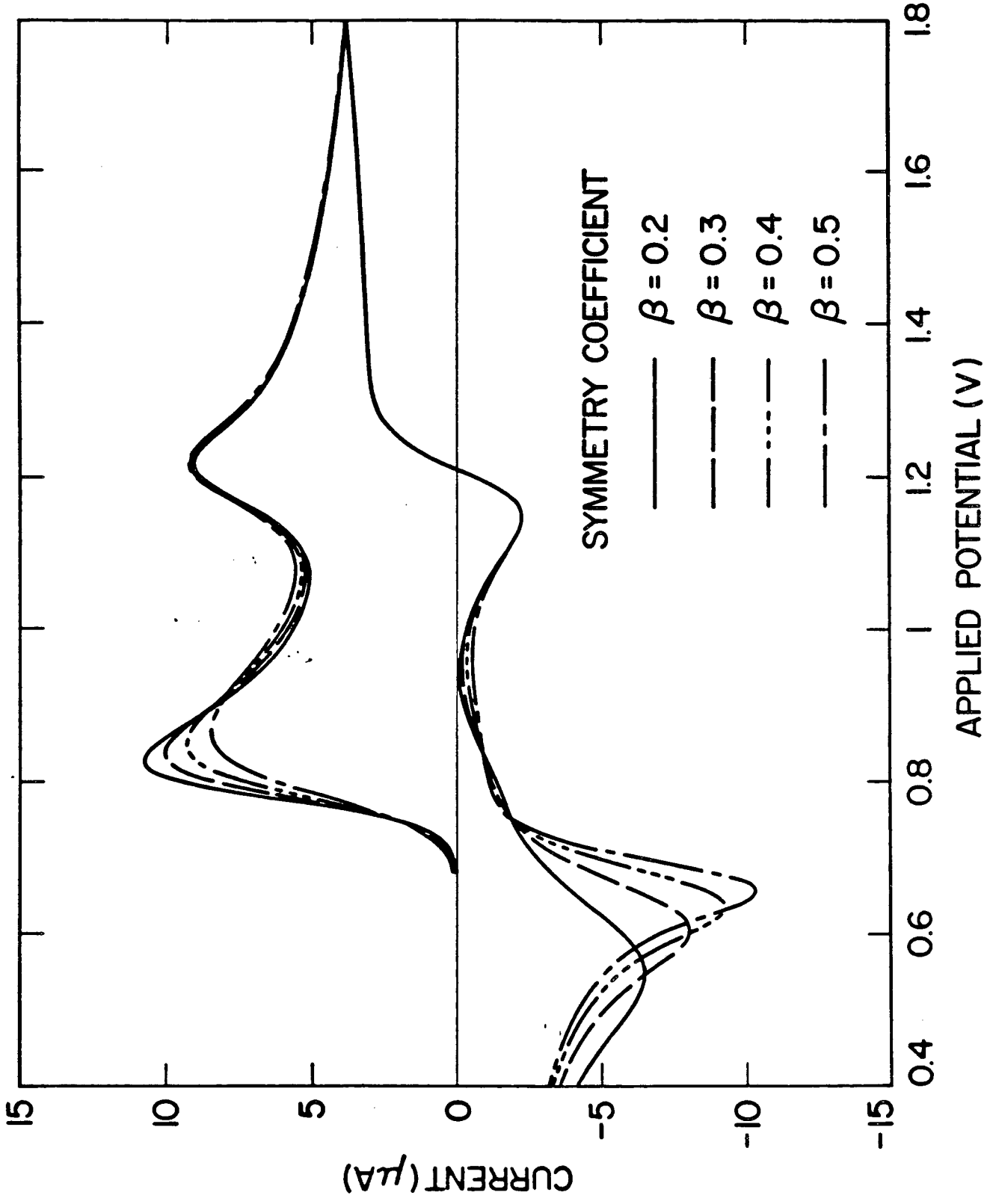
CURRENT (μA)
15
10
5
0
-5
-10
-15
0.4
0.6
0.8
1
1.2
1.4
1.6
1.8
APPLIED POTENTIAL (V)
SYMMETRY COEFFICIENT
β = 0.2
β = 0.3
β = 0.4
β = 0.5

FIGURE 5

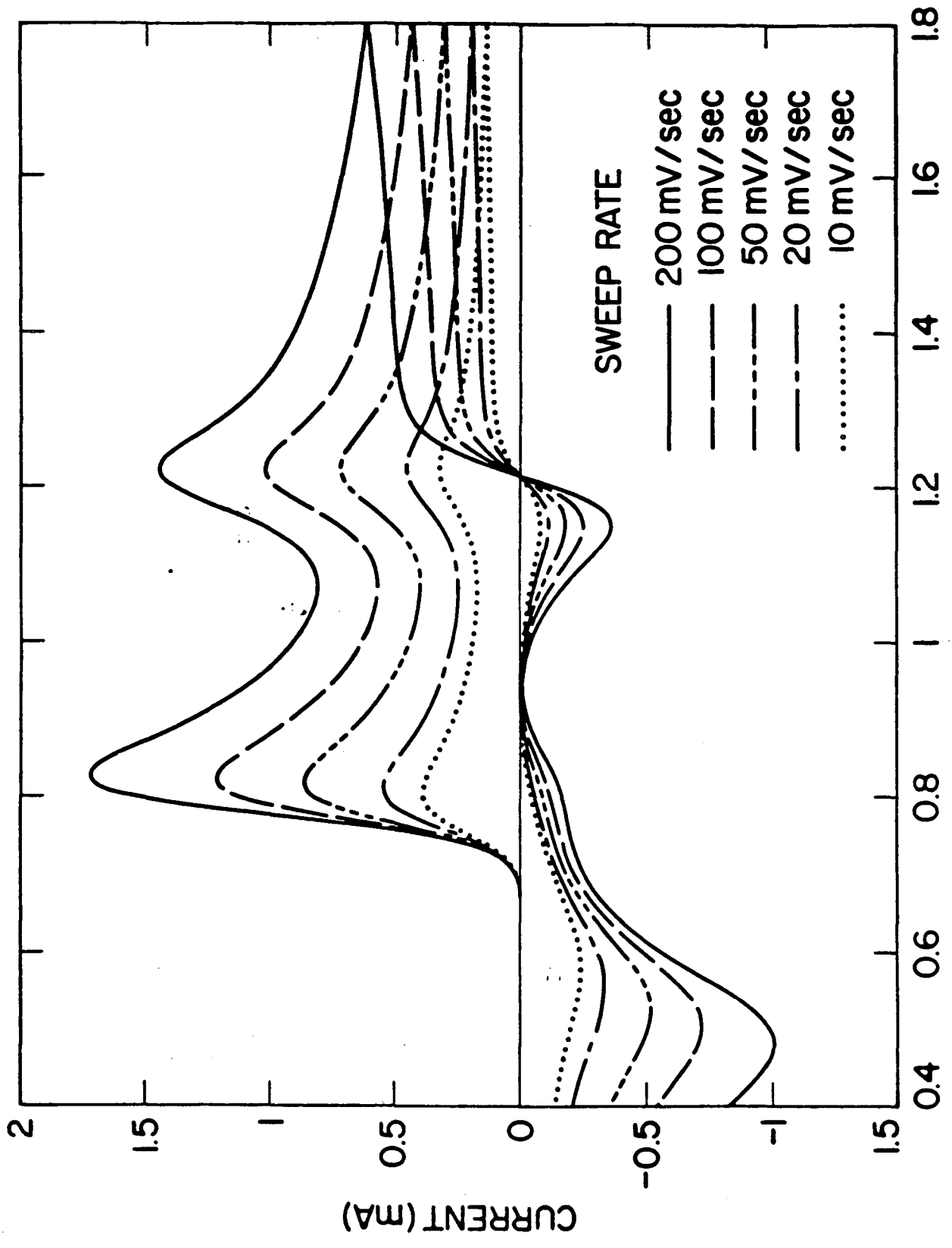
SWEEP RATE
200 mV/sec
100 mV/sec
50 mV/sec
20 mV/sec
10 mV/sec
APPLIED POTENTIAL (V)
CURRENT (mA)
2
1.5
1
0.5
0
-0.5
-1
1.5
0.4
0.6
0.8
1
1.2
1.4
1.6
1.8

FIGURE 6

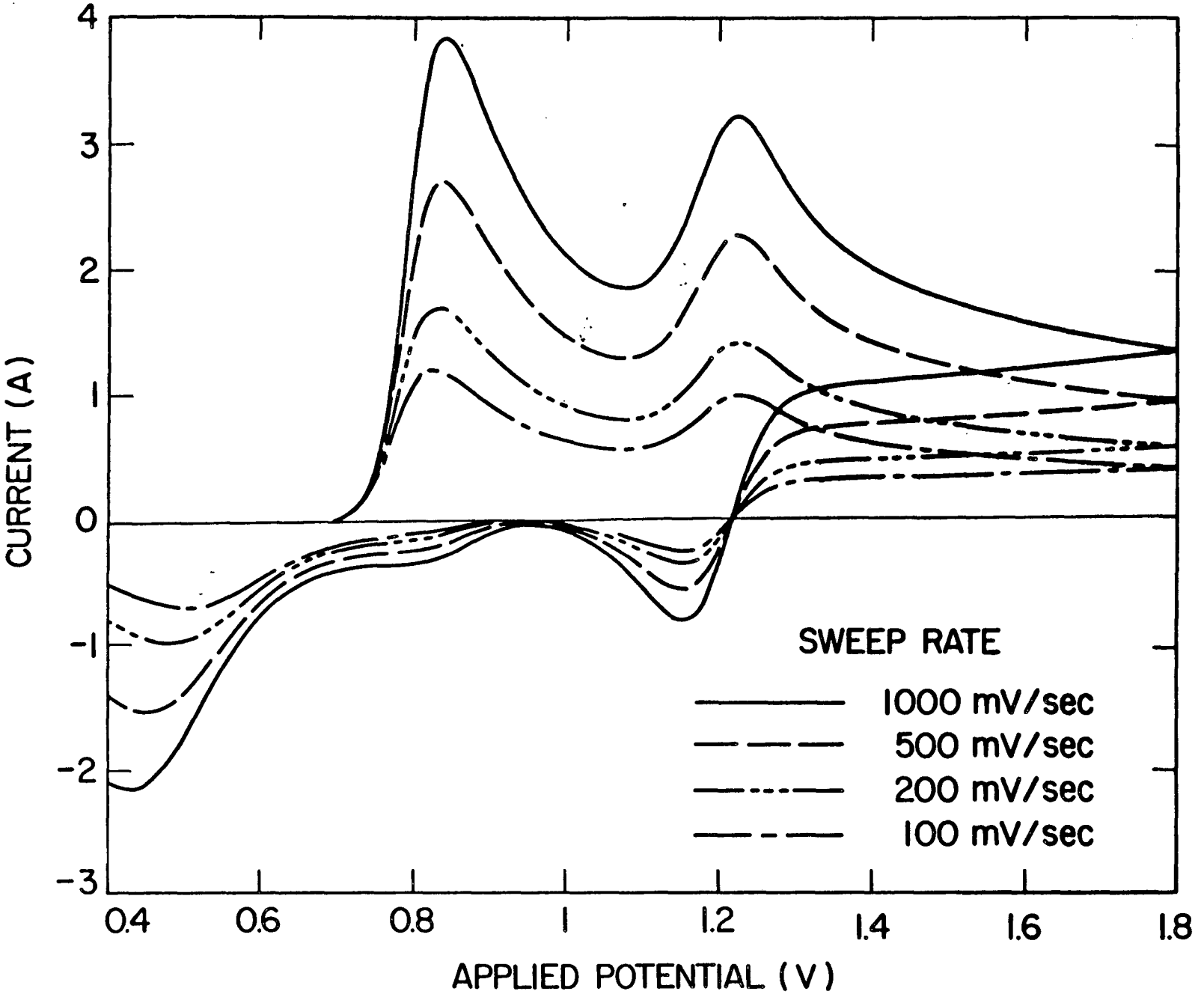
4
3
2
1
0
-1
-2
-3
CURRENT (A)
0.4
0.6
0.8
1
1.2
1.4
1.6
1.8
APPLIED POTENTIAL (V)
SWEEP RATE
1000 mV/sec
500 mV/sec
200 mV/sec
100 mV/sec

FIGURE 7

LAWRENCE BERKELEY LABORATORY
TECHNICAL INFORMATION DEPARTMENT
UNIVERSITY OF CALIFORNIA
BERKELEY, CALIFORNIA 94720